Functional categorization of de novo transcriptome assembly of Vanilla planifolia Jacks. potentially points to a translational regulation during early stages of infection by Fusarium oxysporum f. sp. vanillae

Marco Tulio Solano-De la Cruz
Universidad Nacional Autonoma de Mexico
Jacel Adame-García
Instituto Tecnológico de Úrsulo Galván
Josefat Gregorio-Jorge
Consejo Nacional de Ciencia y Tecnologia
Verónica Jiménez-Jacinto
Universidad Nacional Autonoma de Mexico Instituto de Biotecnologia
Leticia Vega-Alvarado
Universidad Nacional Autonoma de Mexico Instituto de Ciencias Aplicadas y Tecnología
Lourdes Georgina Iglesias-Andreu
Universidad Veracruzana Instituto de Biotecnologia y Ecologia Aplicada
Esteban Elías Escobar-Hernández
Centro de Investigación y de Estudios Avanzados Unidad Irapuato
Mauricio Luna-Rodríguez (mluna@uv.mx)
https://orcid.org/0000-0002-1204-9608

Research article

Keywords: translational regulation, biological defense, transcriptional reprogramming, biotic stress, ribosomal proteins.

Posted Date: October 15th, 2019

DOI: https://doi.org/10.21203/rs.2.12054/v2

Version of Record: A version of this preprint was published on November 8th, 2019. See the published version at https://doi.org/10.1186/s12864-019-6229-5.

Abstract

Background Upon exposure to unfavorable environmental conditions, plants need to respond quickly to maintain their homeostasis. For instance, physiological, biochemical and transcriptional changes occur during plant-pathogen interaction. In the case of Vanilla planifolia Jacks., a worldwide economically important crop, it is susceptible to Fusarium oxysporum f. sp. vanillae (Fov). This pathogen causes root and stem rot (RSR) in vanilla plants that lead to plant death. To investigate how vanilla plants, respond at the transcriptional level upon infection with Fov, here we employed the RNA-Seq approach to analyze the dynamics of whole-transcriptome changes during two-time frames of the infection. Results Analysis of global gene expression profiles upon infection by Fov indicated that the major transcriptional change occurred at 2 days post-inoculation (dpi), in comparison to 10 dpi. Briefly, the RNA-Seq analysis carried out in roots found that 3420 and 839 differentially expressed genes (DEGs) were detected at 2 and 10 dpi, respectively, as compared to the control. In the case of DEGs at 2 dpi, 1563 genes were found to be up-regulated, whereas 1857 genes were down-regulated. Moreover, functional categorization of DEGs at 2 dpi indicated that up-regulated genes are mainly associated to translation, whereas down-regulated genes are involved in cell wall remodeling. Among the translational-related transcripts, ribosomal proteins (RPs) were found increased their expression exclusively at 2 dpi. Conclusions The screening of transcriptional changes of V. planifolia Jacks upon infection by Fov provides insights into the plant molecular response, particularly at early stages of infection. The accumulation of translational-related transcripts at early stages of infection potentially points to a transcriptional reprogramming coupled with a translational regulation in vanilla plants upon infection by Fov. Altogether, the results presented here highlight potential molecular players that might be further studied to improve Fov-induced resistance in vanilla plants.

Background

Throughout evolution, plants have developed multiple defense strategies to cope with pathogens. The first defense line consists of pre-existing physical and chemical barriers, which restrict their entry [1]. In addition to these constitutive barriers, plants have developed an immune response mechanism that is based on the detection of elicitor compounds derived from pathogens, known as Pathogen-Associated Molecular Patterns (PAMPs) [2]. Such defense response activated by the PAMPs or PAMP-Triggered Immunity (PTI), usually restricts the proliferation of the pathogen [3; 4; 5; 6; 7]. However, some pathogens have circumvented this response by developing effector proteins that interfere or suppress PTI [8; 9; 10]. In this sense, the so-called co-evolutionary 'arms race' between plants and pathogens has defined the establishment of the Effector-Triggered Immunity (ETI), a defense line that begins with the recognition of PAMPs by plant pattern recognition receptors (PRRs) [11]. The signals generated by PRRs are transduced through Mitogen-activated Protein Kinases (MAPKs), which in turn activate transcription factors for gene regulation that leads to a proper plant defense response [12]. Among the plant responses, the Hypersensitive Response (HR), the programmed cell death, the expression of proteins related to pathogenesis or the lignification of the cell wall are included [13; 14; 15; 16; 17; 18].

Vanilla planifolia Jacks. is one of the most economically relevant orchids. It is produced extensively in several countries and is the main natural source of one of the most widely used flavoring agents in the world, vanillin [19; 20]. Its cultivation has spread throughout the world, with Madagascar and Indonesia as the leaders of annual production (35.5% and 34.5%, respectively), followed by China (13.7%) and Papua New Guinea (4.1%) [21; 22; 24; 25; 26]. Although Mexico is the center of domestication and diversification of this crop, vanillin production is positioned in the fifth place, contributing to only 4.0% of world production [20]. Importantly, vanilla plants are susceptible to parasites and pathogens. The most lethal pathogen that afflicts vanilla is *Fov*, a pathogenic form of the genus *Fusarium* that specifically infects this plant species [23; 22; 26]. This pathogen causes RSR, as well as the colonization of vascular tissues that finally leads to plant death. Several studies indicate that *V. planifolia* has a high susceptibility and incidence of *Fov* [27; 26; 28]. For instance, infection of vanilla plants by this pathogen is capable of destroying 65% of the plantation [23; 22; 26]. The lack of genetic variability of *V. planifolia* is another factor that worsens the scenario [29; 30; 23]. Thus, given the economic importance of *V. planifolia*, is mandatory to do an effort to elucidate the overall plant response upon infection by this pathogen, likewise, has been done in other crops [31; 32; 33]. Moreover, since inferences from mRNA expression data are valuable as it reflects changes with a biological meaning, we looked into the transcriptome of *V. planifolia* roots exposed to *Fov*, to figure out the responsive mechanisms at early (2 days after inoculation, 2dpi) and later (10 days after inoculation, 10 dpi) stages of infection. Gene expression profiles indicated that major transcriptional changes occur at 2 dpi. Accordingly, vanilla plants accumulate transcripts associated to several processes, but mostly translational regulation-related transcripts. Thus, this study provides the identification of molecular players in plant-pathogen interaction between *V. planifolia* and *F. oxysporum* f. sp. *vanillae*, particularly a transcriptional reprogramming coupled with a translational regulation. Our study is aimed to understand the response of vanilla plants, which could help to fight the most damaging disease of vanilla caused by *Fov*.

Results

Assembly of the transcriptome of *V. planifolia* roots exposed to *Fov*

The transcriptome of vanilla roots exposed to *Fov* was assessed with Illumina sequencing at 2 and 10 dpi. A total of 12 cDNA libraries were paired-end sequenced using the NextSeq 500 system. Sequencing data of these libraries were obtained corresponding to three biological replicates (control and treatment), covering two frames of time along the infection process (Fig. 1). In brief, six libraries corresponding to control and treatment at 2 dpi, as well as six libraries at 10 dpi, produced more than 204 million reads (Fig. 1). Such data were submitted to the GEO platform of NCBI-GenBank (Accession number: GSE134155). To analyze and compare the dispersion of the treatments with respect to the control samples, PCA analyzes were carried out (Additional file 1: Figure S1; and Additional file 2: Figure S2). Figure S1 corresponds to the treatment and control at 2 dpi, whereas Figure S2 corresponds to the treatment and control at 10 dpi; respectively. Pre-processing of raw sequencing reads was carried out with FastQC, which indicated a good per base quality. The results of the quality analysis applied to the raw data, with FastQC software, are hosted under the following link:

http://www.uusmb.unam.mx/reportes/170308/Project_MTulio.html (Additional file 3: Table S1). Filtering reads that correspond to the pathogen used at 2 and 10 dpi, discarded 5.33% and 39%, respectively. On the other hand, even that control plants were not inoculated with the fungus, 5% (2 dpi) and 6.48% (10 dpi) of reads aligned to the genome of *F. oxysporum* f. sp. *lycopersici*, excluding such reads for subsequent analyzes (Fig. 1). The *de novo* transcriptome assembly of vanilla resulted in about 45,000 transcripts (Additional file 4: Figure S3). The statistics of the transcriptome assembly carried out by TransRate v1.0.3 [34] can be found in Additional file 5 (Table S2) (Accession number: GSE134155). In addition, the results of processing data, which involved sequencing statistics of raw data and filtered data, statistics of the sequence alignments *vs.* the *de novo* transcriptome assembly [35], as well as non-aligned sequences and records of sequences that were cleaned are presented in Additional file 3 (Table S1). The generated transcripts were mapped against the plant databases, using the BUSCO software, obtaining about 99% of complete orthologous. Figure S1 shows the results of the annotation of the vanilla transcriptome with Blast2GO, finding about 11,000 unigenes out of the total 45,000 assembled transcripts (Additional file 4: Figure S3). Among the main functional categories of gene ontology obtained were plant development, plant growth, cell proliferation, signaling, response to stimuli and response to stress. Moreover, counting of reads on the assembled transcripts resulted in approximately 30% of transcripts that fulfilled the counts per million required for the subsequent identification of DEGs. Altogether, the assessment of the transcriptome of *V. planifolia* roots exposed to *Fov* revealed that several plant and cellular processes are impacted during the two frames of time evaluated.

Analysis of gene expression and functional categorization of DEGs at 2 and 10 dpi

For the identification of unigenes with changes in expression levels at 2 and 10 dpi, differential gene expression analysis was carried out using several approaches such as DESeq, DESeq2, NOISeq and EdgeR. For libraries corresponding to 2 dpi, 2310, 1702, 4080 and 3420 DEGs were obtained with DESeq, DESeq2, NOISeq and EdgeR, respectively (Fig. 2) (Additional file 6: Table S3). On the other hand, analysis of DEGs at 10 dpi revealed that 812, 534, 839 and 881 DEGs were obtained with DESeq, DESeq2, NOISeq and EdgeR, respectively (Fig. 2) (Additional file 6: Table S3). As EdgeR is the most popular method and taking into account that this method included the vast majority of DEGs, EdgeR was selected for the subsequent analysis (Fig. 2). In that sense, two lists were obtained, one corresponding to the treatment at 2 dpi containing 3420 DEGs and the other corresponding to the treatment at 10 dpi with 881 DEGs. In the case of DEGs at 2 dpi, 1563 genes were found to be up-regulated, whereas 1857 genes were down-regulated. On the other hand, classification of DEGs at 10 dpi as up- and down-regulated genes, resulted in 250 and 631 genes, respectively. An overview of the transcriptional change at 2 and 10 dpi is shown in Fig. 3. At a glance, subsets of certain DEGs showed contrasting expression profiles if both treatments are compared (Fig. 3).

The lack of reference genome for *V. planifolia* forced to check orthology with available genomes for which annotation is complete. Accordingly, orthologs of Arabidopsis corresponding to DEGs at 2 and 10 dpi were obtained, resulting in 603 and 278 orthologs, respectively (Additional file 7: Table S4). As a first approach to elucidate the putative functions of DEGs at 2 and 10 dpi, gene orthologs were submitted to

MapMan [36]. Pathway analysis of DEGs with P-value cut-off of ≤0.05 was carried out on Arabidopsis pathway genes. Accordingly, 603 (2 dpi) and 278 (10 dpi) DEGs were analyzed with MapMan, from which only 535 and 149 were categorized, respectively (Fig. 4). Visualization of the DEGs assigned to functional categories revealed that orthologs with differential expression at 2 dpi showed most enriched categories than that of 10 dpi (Fig. 4). Remarkably, most of data points contained within the functional categories at 2 dpi were up-regulated genes, whereas down-regulated genes were mostly associated to functional categories at 10 dpi (Fig. 4). Among the most enriched categories, genes encoding products involved in regulation of transcription (27) and protein synthesis (29) were observed in both cases (2 and 10 dpi) (Fig. 4). However, the number of genes associated to those functional categories was contrasting. For instance, whereas only 20 data points were found within the category of protein for DEGs at 10 dpi, 123 were found in the case of data corresponding to 2 dpi (Fig. 4). Other enriched categories at 2 dpi were cell wall (10), lipid metabolism (11), amino acid metabolism (13), secondary metabolism (16) and hormone metabolism (17) (Fig. 4). Thus, the functional categorization of DEGs suggest that the major transcriptional change occurs at early stages of infection, namely at 2 dpi.

To further comprehend the functions of DEGs at 2 and 10 dpi, an analysis according to the enrichment of GO terms was carried out using the orthologs. Such analysis in the platform of agriGO resulted in the main functional categories associated to DEGs at 2 dpi (Table 1), but not for DEGs at 10 dpi. For up-regulated genes at 2 dpi, 18, 4 and 30 categories were significantly enriched, corresponding to biological process (P), molecular function (F) and cellular component (C), respectively (Table 1). In the case of down-regulated genes, 9, 3 and 3 categories were found significantly enriches for P, F and C, respectively (Table 1). A schematic representation of biological processes shown in Table 1 allowed to appreciate that translation and cell wall modification were the main processes overrepresented in up- and down-regulated genes, respectively (Additional file 8: Figure S4). Taken together, the functional categorization of DEGs not only suggests that the major transcriptional change occurs at early stages of infection (2 dpi), but also indicates that up-regulated genes are mainly associated to translation, whereas down-regulated genes are involved in cell wall remodeling.

Functional association networks of DEGs at 2 dpi

Since the functional categorization suggested that DEGs coding for protein-related processes are the most contrasting categories when datasets of 2 and 10 dpi are compared, further inspection was carried out for DEGs at 2 dpi. **S**ince genes encode products that interact each other, a network was generated to look for relationships among DEGs at 2 dpi (Fig. 5). Briefly, out of 309 up-regulated genes at 2 dpi with an ortholog in the Arabidopsis genome, only 282 were recognized by String [37]. Accordingly, most of interactions observed in the network corresponded to experimental data (purple lines) (Fig. 5A). Particularly, a central network was formed, involving 98 genes (nodes), from which most of them (80 nodes) were related to translation (structural constituents of ribosome) (Fig. 5A). For example, genes encoding proteins such as Ribosomal protein S12/S23 (Rps12/s23), Ribosomal protein l24B (Rpl24B), Ribosomal protein s6 (Rps6), Ribosomal protein s13 (Rps13), among others, formed the central network (Table 2). In addition to genes involved in translation, genes associated to development were also found

(Table 2). Among this group, *YODA* (*YDA*), *STEROL METHYLTRANSFERASE 1* (*SMT1*), *EMBRYO DEFECTIVE 2386* (*EMB2386*), *MATERNAL EFFECT EMBRYO ARREST 22* (*MEE22*), and others, were found (Table 2).

On the other hand, for down-regulated genes at 2 dpi, 256 were recognized by String out of 294 submitted genes (Fig. 5B). Also, a central network (49 nodes) was obtained with genes involved mainly in cell cycle, DNA replication and cell wall organization (Fig. 5B) (Table 2). In this case, genes encoding proteins such as Cyclin A1;1 (CycA1;1), Cyclin-dependent kinase B2 (CdkB2), Minichromosome maintenance 3 (Mcm3), Origin recognition complex subunit 3 (Orc3), Cellulose synthase-like protein D5 (Csld5), Cellulose synthase A catalytic subunit 8 (CesA8), Cellulose synthase A catalytic subunit 7 (CesA7), among others, clearly formed a central network (Fig. 5B) (Table 2). Notably, these networks were exclusively for DEGs at 2 dpi, since DEGs corresponding to 10 dpi did not show a clear interaction (Additional file 9: Figure S5). In resume, the generation and visualization of relationships among DEGs at 2 dpi show significantly more interactions than expected. In the case of up-regulated genes, they are mainly associated to ribosome biogenesis and translation as well as in development, whereas down-regulated genes are involved in cell cycle, DNA replication and cell wall organization.

Differential gene expression of ribosome-related proteins at 2 dpi

The finding that mainly proteins involved in ribosome biogenesis and translation (structural constituents of ribosome) were the most significant DEGs at 2 dpi, encouraged to focus on these genes. As observed in Fig. 6, proteins related to ribosome biogenesis and translation were significantly up-regulated in 2 dpi compared to 10 dpi, 72 of which were exclusively expressed in the treatment at 2 dpi. These exclusive genes corresponded to ribosomal proteins, for which a significant increase in their expression pattern was observed only at 2 dpi (Fig. 6). As mentioned before, ribosomal proteins such as Ribosomal protein s12/s23 (Rps12/S23), Ribosomal protein l24B (Rpl24B), Ribosomal protein s6 (Rps6), Ribosomal protein s13 (Rps13), among others, were found up-regulated at 2 dpi. In summary, ribosomal-related proteins are found up-regulated at 2 dpi, suggesting that translation is impacted upon infection by *Fov*.

Discussion

As supported by several studies around the world, *Fov* is the principal species that causes RSR in vanilla plants [26; 38; 39]. Although the generation and use of resistant varieties are the best mean to restrict *Fov*, scarce information about the plant-pathogen interaction, as well as limited genetic resources, have impeded to eradicate or limit the devastation that cause *Fov* in vanilla production. Under such scenario, the understanding of mechanistic responses of vanilla plants upon infection by *Fov* is scarce and necessary. Therefore, the primary goal of this work was to elucidate the early and late mechanistic responses of vanilla plants induced by *Fov* through investigating whole transcriptional changes in root tissues (Fig. 1). The RNA-Seq technique was employed to detect the DEGs during two frame times of infection by this root-infecting fungal pathogen, namely at early (2 dpi) and late (10 dpi) stages. The RNA-Seq analysis carried out in roots revealed that 4480 and 881 genes were differentially modulated by *Fov*

at 2 and 10 dpi, respectively, as compared to the control (Fig. 2). This result indicated that the major transcriptional change occurs at early stages of infection, encouraging further analysis for these DEGs (Fig. 3). After functional classification of DEGs at 2 and 10 dpi, it was further confirmed that only DEGs at 2 dpi contained enriched functional categories (Fig 4). For instance, enrichment analyses revealed the involvement of DEGs at 2 dpi to ribosome biogenesis and translation for up-regulated genes, whereas down-regulated genes were mainly associated to cell wall biogenesis (Table 1).

Most biological processes, from cell differentiation to organ development, as well as the adaptation to the environment, relies on transcriptional adjustments. Even that gene expression regulation is solidly established, it is clear that regulation beyond this level also plays a pivotal role in modulating key biological processes. Among the enriched functional categories for DEGs at 2 dpi, translation was the most prominent among up-regulated genes (Table 1) (Additional file 8: Figure S5), suggesting that this biological process is significantly impacted upon infection by *Fov*. Moreover, the formation a single network involving all these RPs supports a putative function in the early stages of infection by *Fov* (Fig. 5A). On the other hand, the finding that down-regulated genes are mostly involved in cell wall modifications (Table 1), is in agreement with the known susceptibility of *V. planifolia* plants to *Fov*. In this regard, since the plant cell wall acts as an important barrier against pathogen penetration by activating cell wall strengthening-related genes [40], the down-regulation of these genes reflects the facilitation of pathogen entry and then the negative impact on processes such as cell division and DNA replication of plant cells (Fig. 5B).

Being the basic infrastructure for protein translation, ribosomal proteins (RPs) have been known primarily for their housekeeping functions [41]. However, in the recent years, emerging functions of RPs have been described, including regulation of gene expression through translational mechanisms [42; 43]. One hint for this is, for example, that even there are at least 230 genes encoding RPs in the Arabidopsis genome, a single member of each family of RPs has been found as part of the subunits of ribosomes, suggesting that expression of the additional RPs are subjected to different cues, including environmental conditions [44; 45]. Among the up-regulated RPs found in this work, *RPL13* has been related to the tolerance of potato to *Verticullum dahliae* [46]. Similarly, *RPL10*, *RPS12/S23*, and *PRPL19e* [47; 48], as well as the expression of *RPS6*, *RPL19*, *RPL7*, and *RPS2* [49], have been associated to plant response against bacteria and virus; respectively. Also, *RPS10* and *RPS10p/S20e* have been found to be up-regulated by *Phytophthora sojae* in *Glycine max* [50]. Finally, *RPL12* and *RPL19* also have been shown to participate in the resistance against *P. syringae* in *Nicotiana benthamiana* and *A. thaliana*, respectively [48; 51]. On the other hand, abiotic stress has also been found to induce transcription of RPs. For example, transcript levels of *RPS15a* (and its variants A, C, D and F) increased significantly in response to heat stress in Arabidopsis [52]. This was also the case for *RPS14*, *RPL13*, and *RPL30* in Arabidopsis, in which their expression levels augment under the treatment with benzylaminopurine [53]. In addition, *RPL10* and *RPL10C* were induced when Arabidopsis plants were treated with UV, like those results obtained in maize plants [54; 55]. Finally, regarding low temperature conditions, increase of *RPS6*, *RPS13* and *RPL37* have been observed in *Glycine max* and *Brassica napus* [56; 57]. Besides the association of these RPs to biotic or abiotic stresses, functional characterization of them has allowed to elucidate their role in plants. In that

sense, mutation of *RPL10* causes lethality of the female gametophyte in Arabidopsis [58]. Also, the mutation of *RPS13A* results in a reduction of cell division, retardation of flowering, and delayed growth of shoots and leaves [59]. Similar phenotypes of growth retardation and fertility reduction have been reported in the *RPL23aA* mutant [60].

In summary, until now, the central role of RPs in development as their global participation in response to abiotic stress in iron and phosphate deficit conditions has been assessed. Here, we report for the first time the RPs global participation in response to biotic stress in a translational manner.

Since translation of proteins is energetically a demanding process, stress can cause a global drop of protein synthesis in plants. However, a translational regulation mechanism leading to the translation of certain transcripts to produce specific RPs [41]. Such regulation mediated by specific RPs may be the key to the survival of plants under stressful conditions [41]. Only in recent years this kind of regulation beyond the transcriptional level has received special interest due to its implications in key biological processes, particularly those related to biotic and abiotic stress responses [42; 43, 61]. Thus, the up-regulation of several RPs during early stages of infection by *Fov* in vanilla plants represent a whole response of translational regulation (Fig. 7), as known about of regulation of translational factors and their associated proteins with translational regulation [61]. In the transcriptional profile of vanilla plants at 2 dpi, induction of *RPL24B*, *RPS18*, *RPS5* and *RPL27A* were found. Since *RPL24B* of Arabidopsis is related to the translation regulation of some auxin signaling genes that contains uORFs [62, 63], the up-regulation of this RP in vanilla plants could suggest the presence of a similar mechanism. Supporting this hypothesis, mutants of *RPL24B*, as well as *RPS18A*, *RPS5B*, *RPS13B* and *RPL27A*, known as "pointed first leaf" mutants, show defective phenotypes related to development, such as the reduction of the growth of shoots and roots [64; 59; 65; 66]. This suggests that, these proteins carry out specific functions during plant development, likely by translating specific transcripts. Accordingly, RPS6, which is responsive to biotic and abiotic stresses, is also a regulator of translation [67]. Specifically, phosphorylation of RPS6 through the TOR signaling pathway lead to the selective translation of mRNAs [41; 61]. Besides RPS6 phosphorylation, phosphorylation of eIF2α by the Gcn2-Gcn1 complex reduces global protein synthesis, which has implications for growth and development [68, 69; 70; 71; 72]. Since *GCN1*, *GCN2* and *EIF2α* were exclusively found in DEGs at 2 dpi and its expression resulted to be high (near to 12 log2 fold change), this suggest, same as in abiotic and biotic stress [73], that the general translation can be decreased, accompanied by selective translation through changes of ribosome composition as the response to pathogen infection.

Under such scenario, upon infection by *Fov*, root cells of vanilla plants likely change the expression of RPs, resulting in alterations of ribosomes composition, as reported against abiotic stress [74] and, therefore, in modulation of translation for certain transcripts as a response of fungal invasion (Fig. 7). This is particularly relevant since this is the first time that RPs are associated to *Fov*-derived response in vanilla plants. Moreover, it has been indicated that the typical chromosomal number of *V. planifolia* is 2n = 32 and more recently, cytogenetic studies conducted in the Mansa morphotype, reported an intra-individual variation in the number of chromosomes in the apical cells of the root, which may vary from 2n

= 20 to 2n = 32 or more. Likewise, the existence of a "progressively partial endoreplication" in *V. planifolia* has been reported, however, this process does not occur in all tissues and some studies have reported that less than half of the genome of *V. planifolia* is being replicating effectively in each cycle. However, we consider that the methodology used in this study minimizes the effect of this phenomenon, so we propose the role of the translational regulation in the early plant response in the interaction with pathogen [75].

Conclusions

The screening of transcriptional changes of *V. planifolia* upon infection by *F. oxysporum* f. sp. *vanillae* shows that the major change occurs at early stages of infection, according to the analysis of DEGs at 2 dpi that shows, among other biological processes, the transcription of RPs increases specifically at this moment. Moreover, given the changes of these RPs are involved in plant developmental programs, as well as in response to biotic and abiotic stress conditions, their differential expression point to a biological role during infection. Therefore, is proposed that in response to *Fov* infection, root cells of vanilla plants activate a transcriptional reprogramming coupled with a translational regulation. The results presented here highlight key processes and potential molecular players that might be further studied to develop vanilla breeding programs, help to fight the most damaging disease of this crop.

Methods

Plant material

From plants of *V. planifolia* Jacks. (Mansa morphotype) growing on a farm located in the Totonacapan region (Veracruz, Mexico), samples were collected and propagated under greenhouse conditions. Vigorous and pathogen-free plants were used in the present study at the developmental age of 12 weeks for infectivity assays. Such plants exhibited leaf morphology characteristic of *V. planifolia*. Sixty plants were distributed in twelve groups of five each one, for an experimental design intended for four treatments (two times conditions and two control) and three biological replicates by treatment (Fig. 1). The time conditions were 2 dpi (2 days post-inoculate) and 10 dpi (10 days post-inoculate) and the controls were plants non-treated with *Fov*.

Infectivity assays

The *in vitro* fungal infection of *V. planifolia* plants was carried out with the JAGH3 strain of *Fov*. This strain of *Fov* was isolated from *V. planifolia* (Mansa morphotype) with evident RSR [76], its pathogenic capacity was proven, so it has been used for further studies [26, 39, 77]. Briefly, cuttings of *V. planifolia* were subjected to darkness for ten days. The absence of light exposition allowed the generation of new roots. A mechanical incision was made in each root under aseptic conditions. Then, roots were exposed to an aqueous solution of spores with a concentration of 1 x 10^6 CFU of *Fov* (JAGH33 strain). The inoculation was carried out directly on the substrate where cuttings were established. Cuttings belonging

to the control group were treated similarly, exposing them to an aqueous solution free of spores. For a single biological experiment, control and treatment experiments consisted of 30 plants of the same age, established on substrate and maintained under greenhouse conditions with a 12-hour photoperiod (shaded). Two biological experiments were carried out covering two frames of time of *Fov* infection, namely 2 and 10 days post-inoculation (dpi) (Fig. 1). For each of the treatments and their respective controls, five tissue samples were collected in each case, pooled and processed immediately for RNA extraction. In total, twelve pools were obtained, covering two biological experiments for each treatment time (2 and 10 dpi).

Total RNA extraction

For the total RNA extraction from the roots of vanilla plants, a protocol was standardized based on a previous report [78]. Briefly, 200 mg of root tissue were homogenized with the Trizol reagent and then treated with Phenol:Chloroform:Isoamyl Alcohol (25:24:1), followed by vortexing and centrifugation. The upper aqueous phase was transferred into silica columns included in the SV Total RNA Isolation System extraction kit from Promega. The integrity of the obtained RNA was determined by electrophoresis in 2% agarose gel, stained with ethidium bromide (EtBr 0.5 ug ml^{-1}) under denaturing conditions. The concentration of total RNA samples was verified using a NanoDrop spectrophotometer, as well as its RNA Integrity Number (RIN) values were obtained with an Agilent 2100 Bioanalyzer system (Agilent Technologies). RNA samples with RIN values >6 were used for cDNA synthesis and subsequent sequencing.

Generation and sequencing of cDNA libraries

The generation and sequencing of the cDNA libraries was carried out in the University Unit of Massive Sequencing and Bioinformatics of the Institute of Biotechnology of the National Autonomous University of Mexico (UUSMB IBT-UNAM). In total, the construction of 12 cDNA libraries was carried out. Afterwards, the sequencing of the cDNA libraries was performed using the Nextseq 500 illumina platform, generating paired-end reads of 76 bp. In total, 204 million 517 thousand 080 reads were obtained.

De novo transcriptome assembly and annotation

Quality of reads obtained from the high-throughput sequencing was carried out using the FastQC software (https://www.bioinformatics.babraham.ac.uk/projects/fastqc/). Reads above 32 nt, without the presence of adapters were considered for further analysis. First, to filter and discard reads corresponding to the plant pathogen used in the infectivity assays, alignment of reads was performed with the Smalt software (version 0.7.6) using the reference genome of *F. oxysporum* f. sp. *lycopersici* strain Fol4287. Then, de novo transcriptome assembly corresponding to *V. planifolia* reads was made using the Trinity software (version 2.4). For assessing the quality of the obtained transcriptome assembly, metrics like total number of contigs, longest contig length, mean and median contig length, and N50 were calculated using TransRate, followed by an analysis with BUSCO to explore completeness according to conserved ortholog content. The analysis with the BUSCO software was carried out using the Liliopsida odb10*

database, following the software default parameters [79]. Subsequently, the annotation of the transcriptions was made with the Trinotate software. The search for the open reading frames in the transcriptions was made with the TransDecoder software. Transcripts and amino acid sequences were aligned against the UniProt database using Blastn and Blastx. Moreover, the presence of PFAM domains in the protein sequences predicted from the transcripts was tested with the HMMER software. Finally, the annotation of the transcripts was done using Blast2go [80], as well as the databases of Gene Ontology (GO), KEGG, COG.

Differential expression analysis and functional categorization

For assessing differentially expressed genes (DEGs) of the assembled transcripts, a method based on mapping the reads against the assembled transcriptome was done. Such mapping of reads was done with Bowtie2, as part of the Trinity pipeline, followed by an analysis with RSEM. The results obtained by RSEM were submitted to IDEAMEX [81], a website intended for differential expression analysis using several approaches. Specifically, IDEAMEX analysis is based on DESeq [82], DESeq2 [83], NOISeq [84] and EdgeR [85] methods. For selection of DEGs, the following parameters were used: padj <= 0.04, FDR <= 0.04 and prob> = 0.96, and a logFC> = 2. Heatmaps for DEGs were done in R using the ggplot2 package [86]. From the functional annotation of the assembled transcripts obtained by Blast2GO, visualization of the transcriptome regarding expression patterns was performed with Mapman V2 software [36]. For functional categorization, DEGs were submitted to the agriGO v2.0 software [87], selecting the singular enrichment analysis (SEA). Finally, gene networks among DEGs were obtained with the STRING software [37].

List Of Abbreviations

RNA-Seq: High-throughput sequencing of RNA.

RPS: Small Subunit of Ribosomal Protein

RPL: Large Subunit of Ribosomal Protein

eiFs: Eukaryotic Initiation Factors

GCN: GENERAL CONTROL NON-DEREPRESSIBLE

logFC: log2 of fold change

Declarations

Ethics approval and consent to participate

Not applicable

Consent for publication

Not applicable

Availability of data and material

The datasets used and/or analyzed during the current study are available from the corresponding author on reasonable request and they were submitted to the GEO platform of NCBI-GenBank (Accession number: GSE134155).

Competing interests

The authors declare that they have no competing interests

Funding

This work was funded by Tecnológico Nacional de México (project number 5911.16-P Transcriptome of *Vanilla planifolia* Jacks., exposed to infection caused by *Fusarium oxysporum* f. sp. *vanillae*). The funders had no role in study design, data collection and analysis, decision to publish, or preparation of the manuscript.

Author´s contributions

MTSC, JAG, LGIA and MLR conceived and designed the experiments. MTSC and EEEH performed the experiments and collected samples. VJJ, LVA, MTSC, EEEH and JGJ performed primary data analysis and carried out bioinformatics analysis. MTSC, JGJ and MLR conceived and organized the manuscript structure. All authors contributed during the manuscript preparation and approved the final manuscript.

Acknowledgements

MTSC gratefully acknowledges to the Consejo Nacional de Ciencia y Tecnología (CONACYT) for the scholarship provided (259580) and to the Tecnológico Nacional de México for financial support of this work. Also, thanks to the Biologist Lolvin Delaurens-Santacruz for his help during the experiments, as well as Dr. Alejandro Blanco, Dr. Gastón Jiménez-Contreras and Dr. Matías Baranzelli for their valuable help, generous support and encouragement during the preparation this manuscript. Finally, we appreciate the technical assistance during RNA extractions to Edder Darío Aguilar-Méndez, Daniel Abisaí Jerez-Prieto, Dulce Natali Gómez-Hernández and Cecilio Mauricio-Ramos.

References

1. Bani M, Pérez-De-Luque A, Rubiales D, Rispail N. Physical and Chemical Barriers in Root Tissues Contribute to Quantitative Resistance to Fusarium oxysporum f. sp. pisi in Pea. Front Plant Sci. 2018; 9(2):1-16. 2. Shiu SH, Karlowski WM, Pan R, Tzeng YH, Mayer KF, et al. Comparative analysis of the receptor-like kinase family in Arabidopsis and rice. The Plant Cell. 2004; 16: 1220-1234. 3. Zhang J, Zhou

JM. Plant immunity triggered by microbial molecular signatures. Mol Plant. 2010; 3: 783-793. doi:10.1093/mp/ssq035. 4. Bigeard J, Rayapuram N, Pflieger D, Hirt H. Phosphorylation-dependent regulation of plant chromatin and chromatin-associated proteins. Proteomics. 2014; 14, 2127-2140. doi: 10.1002/pmic.201400073. 5. Ausubel FM. Are innate immune signaling pathways in plants and animals conserved? Nat. Immunol. 2005; 973-979. 6. Boller T, Felix G. A renaissance of elicitors: perception of microbe-associated molecular patterns and danger signals by pattern-recognition receptors. Annual Review of Plant Biology. 2009; 60: 379-406. 7. Yamaguchi Y, Huffaker A, Bryan AC, Tax FE, Ryan CA. PEPR2 is a second receptor for the Pep1 and Pep2 peptides and contributes to defense responses in Arabidopsis. Plant Cell. 2010; 508-522. 8. Macho AP, Zipfel C. Targeting of plant pattern recognition receptor triggered immunity by bacterial type III secretion system effectors. Current Opinion in Microbiology. 2015; 23: 14-22. 9. Guo M, Tian F, Wamboldt Y, Alfano JR. The majority of the type III effector inventory of Pseudomonas syringae pv. tomato DC3000 can suppress plant immunity. Mol Plant Microbe Interact. 2009; 22: 1069-1080. 10. Zipfel C. Plant pattern-recognition receptors. Trends Immunol. 2014; 35: 345-351. 11. Jones JD, Dangl JL. The plant immune system. Nature. 2006; 444: 323-329 12. Chen X, Ronald PC. Innate immunity in rice. Trends Plant Sci. 2011; 451-459. 13. Whitmarsh AJ. Regulation of gene transcription by mitogen-activated protein kinase signaling pathways. Biochim Biophys Acta - Mol Cell Res. 2007;1773(8):1285-1298. 14. Chiang YH, Coaker G. Effector triggered immunity: NLR immune perception and downstream defense responses. Arabidopsis Book. 2015; 13:e0183 15. Spoel SH, Dong X. How do plants achieve immunity? Defense without specialized immune cells. Nature Reviews Immunology. 2012; 12(2): 89-100. doi: 10.1038/nri3141 16. Naito K, Ishiga Y, Toyoda K, Shiraishi T, Ichinose Y. N-terminal domain including conserved flg22 is required for flagellin-induced hypersensitive cell death in Arabidopsis thaliana. J. Gen. Plant Pathol. 2007; 73: 281-285 17. Clough SJ, Fengler KA, Yu IC, Lippok B, Smith RK, Bent AF. The Arabidopsis dnd1 “defense, no death” gene encodes a mutated cyclic nucleotide-gated ion channel. Proc. Natl. Acad. Sci. U.S.A. 2000; 97: 9323-9328. doi: 10.1073/pnas.150005697 18. Coll NS, Epple P, Dangl JL. Programmed cell death in the plant immune system. Cell Death Differ. 2011; 18: 1247-1256. 19. Anilkumar A. Vanilla cultivation, A profitable agri-based enterprise. Kerala Calling. 2004; 11: 26-30. 20. Hernández-Hernández J. Vanilla Diseases. In: Handbook of Vanilla Science and Technology. London, United Kingdom: Wiley-Blackwell Publishing. 2011; 27-39. 21. De La Cruz Medina J, Rodriguez Jiménes GC, García HS. VANILLA Postharvest Operations. Post-harvest Compendium. 2009. 22. Kalimuthu K, SenThilkumar R, Vilayakumar S. In vitro micropropagation of orchid, Oncidium sp. (Dancing Dolls). African Journal of Biotechnology. 2007; 6(10): 1171-1174. 23. Dignum MJW, Kerler J, Verpoorte R. β-Glucosidase and peroxidase stability in crude enzyme extracts from green beans of Vanilla planifolia Andrews. Phytochemical Analysis. 2001; 12: 174-179. 24. Roling W, Kerler J. Microorganisms with a taste for vanilla:microbial ecology of traditional indonesian vanilla curing. applied and enviromental microbiology. 2001; 5(67): 1995-2002. 25. Pinaria A, Burgess L. Fusarium species associated with vanilla stem rot in Indonesia. Australasian Plant Pathology. 2010; 39: 83-176. 26. Ramírez-Mosqueda M., Iglesias-Andreu L., Noa-Carrazana J, Armas-Silva A. Selection of Vanilla planifolia Jacks. ex Andrews genotypes resistant to Fusarium oxysporum f. sp. vanillae, by biotechnology. Agroproductividad. 2018; 11: 70-74. http://www.revista-agroproductividad.org/index.php/agroproductividad/article/view/219/162 27. Bhai S, Dhanesh J.

Occurrence of fungal diseases in vanilla (Vanilla planifolia Andrews) in Kerala. Journal of Spices and Aromatic Crops. 2008; 17: 140-148. 28. Fravel D, Olivain C, Alabouvette C. Fusarium oxysporum and its biocontrol. New Phytologist. 2003; 157: 493-502. 29. Bory S, Lubinsky P, Risterucci AM, Noyer JL, Grisoni M, Duval MF, Besse P. Patterns of introduction and diversification of Vanilla planifolia (Orchidaceae) in Réunion Island (Indian Ocean). American Journal of Botany. 2008; 95: 805-815 30. Lubinsky P, Bory S, Hernández JH, Kim SC, Gómez-Pompa A. Origins and dispersal of cultivated Vanilla (Vanilla planifolia Jacks. [Orchidaceae]). Economic Botany. 2008; 62: 127-138. 31. Bai TT, Xie WB, Zhou PP, et al. Transcriptome and Expression Profile Analysis of Highly Resistant and Susceptible Banana Roots Challenged with Fusarium oxysporum f. sp. cubense Tropical Race 4. PLoS ONE. 2013; 8(9): e73945. doi: 10.1371/journal.pone.0073945. 32. Li CY, Deng GM, Yang J, Viljoen A, Jin Y, Kuang RB, Zuo CW, Lv ZC, Yang QS, Sheng O, Wei YR, Hu CH, Dong T, Yi GJ. Transcriptome profiling of resistant and susceptible Cavendish banana roots following inoculation with Fusarium oxysporum f. sp. cubense tropical race 4. BMC Genomics. 2012; 13: 374. doi: 10.1186/1471-2164-13-374. 33. Xing M, Lv H, Ma J, Xu D, Li H, Yang L, et al. Transcriptome Profiling of Resistance to Fusarium oxysporum f. sp. conglutinans in Cabbage (Brassica oleracea) Roots. PLoS ONE. 2016; 11(2): e0148048. doi: 10.1371/journal.pone.0148048 34. Smith-Unna R, Boursnell C, Patro R, Hibberd JM, Kelly S. TransRate:reference free quality assessment of de novo transcriptome assemblies.Genome Res. 2016;26:1134–4. 10.1101/gr.196469.115 10.1101/gr.196469.115 35. Langmead B and Salzberg, SL. Fast Gapped-Read Alignment with Bowtie 2. Nature Methods. 2012; 9, 357-359. http://dx.doi.org/10.1038/nmeth.1923 36. Thimm O, Bläsing O, Gibon Y, Nagel A, Meyer S, Krüger P, et al. MAPMAN: A user-driven tool to display genomics data sets onto diagrams of metabolic pathways and other biological processes. Plant J. 2004; 37(6): 914-939. 37. Szklarczyk D, Morris JH, Cook H, Kuhn M, Wyder S, Simonovic M, et al. The STRING database in 2017: Quality-controlled protein-protein association networks, made broadly accessible. Nucleic Acids Res. 2017; 45(D1): D362-D368 38. Vijayan K, Srivastava PP, Raju PJ, Saratchandra B. Breeding for higher productivity in mulberry. Czech J. Genet. Plant Breed. 2012. 48: 147-156. 39. Ramírez-Mosqueda MA, Iglesias-Andreu LG, Teixeira da Silva JA. et al. In vitro selection of vanilla plants resistant to Fusarium oxysporum f. sp. vanillae. Acta Physiol Plant. 2019. 41: 40. doi: 10.1007/s11738-019-2832-y 40. Houston K, Tucker MR, Chowdhury J, Shirley N, Little A. The plant cell wall: a complex and dynamic structure as revealed by the responses of genes under stress conditions. Front Plant Sci. 2016; 7: 984. 41. Merchante C, Stepanova AN, Alonso JM. Translation regulation in plants: an interesting past, an exciting present and a promising future. Plant J. 2017; 90(4): 628-653 42. Gonskikh Y, Polacek N. Alterations of the translation apparatus during aging and stress response. Mech. Ageing Dev. 2017; 168: 30-36 43. Warner JR, McIntosh KB. How common are extraribosomal functions of ribosomal proteins? Mol. Cell. 2009; 34: 3-11. doi: 10.1016/j.molcel.2009.03.006. 44. Barakat A, Szick-Miranda K, Chang IF, Guyot R, Blanc G, Cooke R, et al. The organization of cytoplasmic ribosomal protein genes in the Arabidopsis genome. Plant Physiol. 2001; 127: 398-415. doi: 10.1104/pp.010265 45. Perry RP. Balanced production of ribosomal proteins. Gene. 2007; 401: 1-3. 46. Yang L, Xie C, Li W, Ruijie Z, Dengwei J, Qing Y. Expression of a wild eggplant ribosomal protein L13a in potato enhances resistance to Verticillium dahliae. Plant Cell Tissue Organ Cult. 2013; 115: 329-340. doi: 10.1007/s11240-013-0365-4. 47. Falcone Ferreyra ML, Rius S, Emiliani J, Pourcel L, Feller A, Morohashi K, Casati P, Grotewold E. Cloning and characterization of a UV-B

inducible maize flavonol synthase. Plant J. 2010; 62: 77-91. 48. Nagaraj S, Senthil-Kumar M, Ramu VS, Wang K, Mysore KS. Plant Ribosomal Proteins, RPL12 and RPL19, Play a Role in Nonhost Disease Resistance against Bacterial Pathogens. Front. Plant Sci. 2016; 6: 1192. doi: 10.3389/fpls.2015.01192 49. Yang C, Zhang C, Dittman JD, Whitham SA. Differential requirement of ribosomal protein S6 by plant RNA viruses with different translation initiation strategies. Virology. 2009; 390: 163-173. 50. Zhang J, Xia C, Duan C, Sun S, Wang X, Wu X, Zhu Z. Identification and Candidate Gene Analysis of a Novel Phytophthora Resistance Gene Rps10 in a Chinese Soybean Cultivar. PLoS One. 2013; 8(7): e69799. doi: 10.1371/journal.pone.0069799 51. Saha A, Das S, Moin M, Dutta M, Bakshi A, Madhav M, Kirti P. Genome-wide identification and comprehensive expression profiling of ribosomal protein small subunit genes and their comparative analysis with the large subunit genes in rice. Front Plant Sci. 2017; 15; 8: 1553. doi: 10.3389/fpls.2017.01553. 52. Hulm JL, McIntosh KB, Bonham-Smith PC. Variation in transcript abundance among the four members of the Arabidopsis thaliana RIBOSOMAL PROTEIN S15a gene family. Plant Sci. 2005; 169: 267-278. doi: 10.1016/j.plantsci.2005.04.001. 53. Cherepneva GN, Schmidt KH, Kulaeva ON, Oelmüller R, Kusnetsov V. Expression of the ribosomal proteins S14 S16 L13a and L30 is regulated by cytokinin and abscisic acid: implication of the involvement of phytohormones in translational processes. Plant Sci. 2003; 165: 925-932. doi: 10.1016/S0168-9452(03)00204-8. 54. Casati P, Virginia W. Gene expression profiling in response to ultraviolet radiation in maize genotypes with varying flavonoid content. Plant Physiol. 2003; 132: 1739-1754. doi: 10.1104/pp.103.022871. 55. Ferreyra MLF, Casadevall R, Luciani MD, Pezza A, Casati P. New evidence for differential roles of l10 ribosomal proteins from Arabidopsis. Plant Physiol. 2013; 163: 378-391. doi: 10.1104/pp.113.223222. 56. Kim KY, Park SW, Chung, YS, Chung CH, Kim JI, Lee JH. Molecular cloning of low-temperature-inducible ribosomal proteins from soybean. J. Exp. Bot. 2004; 55: 1153-1155. doi: 10.1093/jxb/erh125. 57. Sáez-Vásquez J, Gallois P, Delseny M. Accumulation and nuclear targeting of BnC24 a Brassica napus ribosomal protein corresponding to a mRNA accumulating in response to cold treatment. Plant Sci. 2000; 156: 35-46. doi: 10.1016/S0168-9452(00)00229-6. 58. Imai A, Komura M, Kawano E, Kuwashiro Y, Takahashi T. A semi-dominant mutation in the ribosomal protein L10 gene suppresses the dwarf phenotype of the acl5 mutant in Arabidopsis thaliana. Plant J. 2008; 56: 881-890. doi: 10.1111/j.1365-313X.2008.03647.x. 59. Ito T, Gyung-Tae K, Kazuo S. Disruption of an Arabidopsis cytoplasmic ribosomal protein S13-homologous gene by transposon-mediated mutagenesis causes aberrant growth and development. Plant J. 2000; 22: 257-264. doi: 10.1046/j.1365-313x.2000.00728.x. 60. Degenhardt RF, Bonham-Smith PC. Arabidopsis ribosomal proteins RPL23aA and RPL23aB are differentially targeted to the nucleolus and are disparately required for normal development. Plant Physiol. 2008; 147: 128-142. doi: 10.1104/pp.107.111799. 61. Muench DG, Zhang C, Dahodwala M. Control of cytoplasmic translation in plants. Wiley Interdiscip. Rev. RNA. 2012; 3: 178-194. 62. Browning KS and Bailey Serres J. Mechanism of cytoplasmic mRNA Translation. Arabidopsis Book. 2015; 13: e0176. 63. Nishimura EK, Granter SR, Fisher DE. Mechanisms of hair graying: incomplete melanocyte stem cell maintenance in the niche. Science. 2005; 307: 720-724. [PubMed: 15618488] 64. Revenkova E, Masson J, Koncz C, Afsar K, Jakovleva L, Paszkowski J. Involvement of Arabidopsis thaliana ribosomal protein S27 in mRNA degradation triggered by genotoxic stress. 1999; EMBO J. 18: 490-499. doi: 10.1093/emboj/18.2.490. 65. Szakonyi D, Byrne ME. Ribosomal protein L27a is required for growth and patterning in Arabidopsis

thaliana. Plant J. 2011; 65: 269-281. doi: 10.1111/j.1365-313X.2010.04422.x. 66. Horiguchi G, Van Lijsebettens M, Candela H, Micol JL, Tsukaya H. Ribosomes and translation in plant developmental control. Plant Sci. 2012; 191-192: 24-34. 67. Boex-Fontvieille E, Daventure M, Jossier M, Zivy M, Hodges M, Tcherkez G. Photosynthetic control of Arabidopsis leaf cytoplasmic translation initiation by protein phosphorylation. PLoS ONE. 2013; 8: e70692. 68. Zhang Y, Wang Y, Kanyuka K, Parry MAJ, Powers SJ, Halford NG. GCN2-dependent phosphorylation of eukaryotic translation initiation factor-2alpha in Arabidopsis. J. Exp. Bot. 2008; 59: 3131-3141. 69. Liu X, Merchant A, Rockett KS, McCormack M, Pajerowska-Mukhtar KM. Characterization of Arabidopsis thaliana GCN2 kinase roles in seed germination and plant development. Plant Signal. Behav. 2015; 10: e992264. 70. Hannig EM, et al. The translational activator GCN3 functions downstream from GCN1 and GCN2 in the regulatory pathway that couples GCN4 expression to amino acid availability in Saccharomyces cerevisiae. Genetics. 1990; 126(3): 549-562 71. Sormani R, Masclaux-Daubresse C, Daniele-Vedele F, Chardon F. Transcriptional regulation of ribosome components are determined by stress according to cellular compartments in Arabidopsis thaliana. PLoS ONE. 2011; 6: e28070, doi: 10.1371/journal.pone.0028070. 72. Wang L, Li H, Zhao C. et al. The inhibition of protein translation mediated by AtGCN1 is essential for cold tolerance in Arabidopsis thaliana. Plant Cell Environ. 2017; 40: 56-68. 73. Sesma A, Castresana C, Castellano MM. Regulation of translation by TOR, eIF4E and eIF2a in plants: Current knowledge, challenges and future perspectives. Front Plant Sci. 2017; 8: 1-7. 74. Wang J, Lan P, Gao H, Zheng L, Li W, Schmidt W. Expression changes of ribosomal proteins in phosphate-and iron-deficient Arabidopsis roots predict stress-specific alterations in ribosome composition. BMC Genomics. 2013; 14: 783. doi: 10.1186/1471-2164-14-783 75. Bory, S., Catrice, O., Brown, S.C., Leitch, I.J., Gigant, R., Chiroleu, F., Grisoni, M., Duval, M.-F.& Besse, P. (2008). Natural polyploidy in Vanilla planifolia (Orchidaceae) Genome,Vol.51 pp.816-826. 76. Adame-García J, Rodríguez-Guerra R, Iglesias-Andreu LG, Ramos-Prado JM, Luna-Rodríguez M. Molecular identification and pathogenic variation of Fusarium species isolated from Vanilla planifolia in Papantla. Mexico. Bot. Sci. 2015; 93: 669-678. http://dx.doi.org/10.17129/botsci.142 77. Flores-de la Rosa FR, De Luna E, Adame-García J, Iglesias-Andreu LG, Luna-Rodríguez M. Phylogenetic position and nucleotide diversity of Fusarium oxysporum f. sp. vanillae worldwide based on translation elongation factor 1α sequences. Plant Pathology, 2018; 67(6): 1278-1285. doi: 10.1111/ppa.12847 78. Valderrama-Cháirez ML, Cruz-Hernández A, Paredes-López O. Isolation of functional RNA from cactus fruit. Plant Mol. Biol. Rep. 2002; 20: 279-286. 79. Simão FA, Waterhouse RM, Ioannidis P, Kriventseva EV, Zdobnov EM. BUSCO: assessing genome assembly and annotation completeness with single-copy orthologs. Bioinformatics. 2015; 31: 3210. 80. Gôtz S, Garcia-Gomez JM, Terol J, Williams TD, Nagaraj SH, Nueda MJ, Robles M, Talon M, Dopazo J, Conesa A. High-throughput functional annotation and data mining with the blast2go suite. Nucl. Acids Res. 2018. 81. Jiménez-Jacinto V, Sanchez-Flores A, Vega-Alvarado L. Integrative Differential Expression Analysis for Multiple EXperiments (IDEAMEX): A Web Server Tool for Integrated RNA-Seq Data Analysis. Frontiers in Genetics. 2019; 10 (279): 1-16. 82. Anders S, Huber W. Differential expression analysis for sequence count data. Genome Biol. 2010; 11: 106. doi: 10.1186/gb-2010-11-10-r106. 83. Love MI, Anders S, Huber W. Moderated Estimation of Fold Change and Dispersion for Rna-Seq Data with Deseq2. Genome Biology. 2014; 15 (550): 1-21. 84. Tarazona S, Turra D, Furio-Tari P. Data Quality Aware Analysis of Differential Expression in Rna-Seq with Noiseq R/Bioc Package. Nucleic Acids Research.

2015; 43 (21): e140. 85. Robinson MD, Smyth GK, McCarthy DJ. EdgeR: A Bioconductor Package for Differential Expression Analysis of Digital Gene Expression Data. Bioinformatics. 2010; 26 (1): 139-140. 86. Wickham H. A layered grammar of graphics. Journal of Computational and Graphical Statistics. 2009. 87. Tian T, Liu Y, Yan H, You Q, Yi X, Du Z, Xu W, Su Z. agriGO v2.0: a GO analysis toolkit for the agricultural community. 2017; update. Nucleic Acids Res 2017; gkx382. doi: 10.1093/nar/gkx382

Tables

	GO term	Ontology	Description	p-value	FDR
ulated	GO:0006412	P	translation	2.90E-41	2.10E-38
	GO:0034645	P	cellular macromolecule biosynthetic process	6.50E-29	1.90E-26
	GO:0009058	P	biosynthetic process	7.90E-29	1.90E-26
	GO:0009059	P	macromolecule biosynthetic process	1.00E-28	1.90E-26
	GO:0044249	P	cellular biosynthetic process	2.80E-28	4.00E-26
	GO:0019538	P	protein metabolic process	1.10E-26	1.30E-24
	GO:0010467	P	gene expression	1.80E-24	1.90E-22
	GO:0044267	P	cellular protein metabolic process	2.70E-24	2.40E-22
	GO:0044238	P	primary metabolic process	4.00E-24	3.20E-22
	GO:0043170	P	macromolecule metabolic process	6.60E-21	4.70E-19
	GO:0008152	P	metabolic process	1.40E-20	9.10E-19
	GO:0044260	P	cellular macromolecule metabolic process	4.40E-19	2.60E-17
	GO:0044237	P	cellular metabolic process	3.40E-17	1.90E-15
	GO:0009987	P	cellular process	1.60E-16	8.30E-15
	GO:0042254	P	ribosome biogenesis	2.70E-16	1.30E-14
	GO:0022613	P	ribonucleoprotein complex biogenesis	6.60E-16	3.00E-14
	GO:0044085	P	cellular component biogenesis	4.40E-11	1.80E-09
	GO:0009791	P	post-embryonic development	3.90E-06	0.00016
	GO:0003735	F	structural constituent of ribosome	4.20E-57	1.40E-54
	GO:0005198	F	structural molecule activity	5.20E-50	8.30E-48
	GO:0008135	F	translation factor activity, nucleic acid binding	1.20E-07	1.30E-05
	GO:0003746	F	translation elongation factor activity	6.10E-07	4.90E-05
	GO:0022626	C	cytosolic ribosome	4.60E-65	1.00E-62
	GO:0044445	C	cytosolic part	1.00E-	1.10E-

			57	55
GO:0033279	C	ribosomal subunit	5.50E-56	4.10E-54
GO:0005840	C	ribosome	1.20E-55	6.50E-54
GO:0030529	C	ribonucleoprotein complex	2.00E-48	8.80E-47
GO:0043232	C	intracellular non-membrane-bounded organelle	3.70E-45	1.20E-43
GO:0043228	C	non-membrane-bounded organelle	3.70E-45	1.20E-43
GO:0005829	C	cytosol	3.90E-43	1.10E-41
GO:0022625	C	cytosolic large ribosomal subunit	3.20E-40	7.70E-39
GO:0015934	C	large ribosomal subunit	1.10E-35	2.40E-34
GO:0044422	C	organelle part	3.30E-30	6.00E-29
GO:0044446	C	intracellular organelle part	3.20E-30	6.00E-29
GO:0032991	C	macromolecular complex	7.00E-27	1.20E-25
GO:0022627	C	cytosolic small ribosomal subunit	1.20E-22	1.80E-21
GO:0015935	C	small ribosomal subunit	1.10E-20	1.60E-19
GO:0044444	C	cytoplasmic part	2.30E-19	3.20E-18
GO:0005737	C	cytoplasm	2.80E-18	3.70E-17
GO:0005730	C	nucleolus	2.70E-16	3.20E-15
GO:0043229	C	intracellular organelle	4.40E-14	4.90E-13
GO:0005622	C	intracellular	4.40E-14	4.90E-13
GO:0043226	C	organelle	4.70E-14	4.90E-13
GO:0031981	C	nuclear lumen	1.00E-13	1.00E-12
GO:0044424	C	intracellular part	2.70E-13	2.60E-12
GO:0043233	C	organelle lumen	2.20E-12	1.90E-11
GO:0070013	C	intracellular organelle lumen	2.20E-12	1.90E-11
GO:0044428	C	nuclear part	2.50E-12	2.10E-11

	GO:0031974	C	membrane-enclosed lumen	2.80E-12	2.30E-11
	GO:0044464	C	cell part	1.80E-08	1.30E-07
	GO:0005623	C	cell	1.80E-08	1.30E-07
	GO:0016020	C	membrane	7.70E-07	5.60E-06
vn-ated	GO:0042545	P	cell wall modification	2.20E-06	0.00088
	GO:0009664	P	plant-type cell wall organization	1.40E-06	0.00088
	GO:0044262	P	cellular carbohydrate metabolic process	4.70E-06	0.001
	GO:0005975	P	carbohydrate metabolic process	5.00E-06	0.001
	GO:0005976	P	polysaccharide metabolic process	9.60E-06	0.0016
	GO:0006260	P	DNA replication	1.60E-05	0.0021
	GO:0009827	P	plant-type cell wall modification	2.70E-05	0.0032
	GO:0060918	P	auxin transport	5.70E-05	0.0055
	GO:0009914	P	hormone transport	6.20E-05	0.0055
	GO:0003824	F	catalytic activity	1.30E-06	0.00031
	GO:0016757	F	transferase activity, transferring glycosyl groups	7.00E-05	0.0075
	GO:0016758	F	transferase activity, transferring hexosyl groups	9.50E-05	0.0075
	GO:0030312	C	external encapsulating structure	6.70E-07	4.70E-05
	GO:0005618	C	cell wall	5.90E-07	4.70E-05
	GO:0031225	C	anchored to membrane	9.00E-05	0.0042

Protein Name	Protein Identifier	Protein Description
emb2386	AT1G02780.1	Ribosomal protein L19e family protein; Embryo defective 2386 (emb2386)
AT4G39200	AT4G39200.1	Ribosomal protein S25 family protein
BBC1	AT3G49010.3	Encodes 60S ribosomal protein L13
AT1G01100	AT1G01100.2	60S acidic ribosomal protein family
AT2G09990	AT2G09990.1	Ribosomal protein S5 domain 2-like superfamily protein
AT5G15520	AT5G15520.1	Ribosomal protein S19e family protein
AT5G02610	AT5G02610.2	Ribosomal L29 family protein
AT4G10450	AT4G10450.1	Ribosomal protein L6 family
SAG24	AT1G66580.1	Senescence associated gene 24 (SAG24)
PHT3;1	AT5G14040.1	Mitochondrial phosphate carrier protein 3, mitochondrial
AT3G56340	AT3G56340.1	Ribosomal protein S26e family protein
AT4G27090	AT4G27090.1	Ribosomal protein L14
ELF5A-1	AT1G13950.1	Encodes eukaryotic translation initiation factor 5A (EIF-5A)
AT5G02960	AT5G02960.1	Ribosomal protein S12/S23 family protein
AT4G30800	AT4G30800.1	Nucleic acid-binding, OB-fold-like protein
STV1	AT3G53020.1	RPL24B encodes ribosomal protein L24
AT3G07110	AT3G07110.2	Ribosomal protein L13 family protein
AT5G16130	AT5G16130.1	Ribosomal protein S7e family protein
RPL5B	AT5G39740.2	60S ribosomal protein L5-2; Component of the ribosome
AT3G45030	AT5G62300.1	Ribosomal protein S10p/S20e family protein
AT5G02450	AT5G02450.1	Ribosomal protein L36e family protein
AT1G52300	AT1G52300.1	Zinc-binding ribosomal protein family protein
AT1G15930	AT1G15930.1	Ribosomal protein L7Ae/L30e/S12e/Gadd45 family protein
AT2G41840	AT2G41840.1	Ribosomal protein S5 family protein
AT3G28900	AT3G28900.1	Ribosomal protein L34e superfamily protein
AT2G32060	AT2G32060.1	Ribosomal protein L7Ae/L30e/S12e/Gadd45 family protein
AT2G40010	AT2G40010.1	Ribosomal protein L10 family protein

AT2G44120	AT2G44120.2	Ribosomal protein L30/L7 family protein
AT1G74270	AT1G74270.1	Ribosomal protein L35Ae family protein
AT3G06680	AT3G06680.1	Ribosomal L29e protein family
AT5G59850	AT5G59850.1	Ribosomal protein S8 family protein
RPS18C	AT4G09800.1	40S ribosomal protein S18
RPS5A	AT3G11940.1	One of two genes encoding the ribosomal protein S5
AT4G17390	AT4G17390.1	Ribosomal protein L23/L15e family
AT4G34670	AT4G34670.1	Ribosomal protein S3Ae
AT4G36130	AT4G36130.1	Ribosomal protein L2 family
P40	AT1G72370.1	40S ribosomal protein Sa-1
GRP4	AT3G23830.2	Glycine-rich RNA-binding protein 4, mitochondrial
RPL3B	AT1G61580.1	60S ribosomal protein L3-2; R-protein L3 B (RPL3B)
EIF3G1	AT3G11400.2	Eukaryotic translation initiation factor 3 subunit G
AT3G60245	AT3G60245.1	Zinc-binding ribosomal protein family protein
RPS13A	AT4G00100.1	Encodes a cytoplasmic ribosomal protein S13 homologue
AT2G04520	AT2G04520.1	Putative translation initiation factor eIF-1A
AT2G37190	AT2G37190.1	Ribosomal protein L11 family protein; Binds directly to 26S ribosomal RNA
EIF4E	AT4G18040.1	Eukaryotic translation initiation factor 4E-1
AT5G15200	AT5G15200.1	Ribosomal protein S4
AT5G58420	AT5G58420.1	Ribosomal protein S4 (RPS4A) family protein
emb2171	AT3G04400.1	Ribosomal protein L14p/L23e family protein; Embryo defective 2171 (emb2171)
AT3G09630	AT3G09630.1	Ribosomal protein L4/L1 family
AT5G22440	AT5G22440.2	Ribosomal protein L1p/L10e family
NRPC2	AT5G45140.1	DNA-directed RNA polymerase III subunit 2
RPL21A	AT1G09590.1	Translation protein SH3-like family protein
LOS1	AT1G56070.1	Ribosomal protein S5/Elongation factor G/III/V family protein
TRX1	AT3G51030.1	Thioredoxin H-type 1
AT3G04920	AT3G04920.1	Ribosomal protein S24e family protein

AT2G44860	AT2G44860.1	Probable ribosome biogenesis protein RLP24
AT3G24830	AT3G24830.1	Ribosomal protein L13 family protein
AT1G67430	AT1G67430.1	Ribosomal protein L22p/L17e family protein
AT5G59240	AT5G59240.1	Ribosomal protein S8e family protein
AT2G27710	AT2G27710.1	60S acidic ribosomal protein family
AT4G18100	AT4G18100.1	Ribosomal protein L32e; Involved in translation, ribosome biogenesis
AT5G04800	AT5G04800.4	Ribosomal S17 family protein
RPL18	AT3G05590.1	Encodes cytoplasmic ribosomal protein L18
RPL16A	AT2G42740.1	Ribosomal protein large subunit 16A
AT5G67510	AT5G67510.1	Translation protein SH3-like family protein
AT1G70600	AT1G70600.1	Ribosomal protein L18e/L15 superfamily
AT1G74060	AT1G74060.1	Ribosomal protein L6 family protein
RPL23AB	AT3G55280.1	60S ribosomal protein L23A (RPL23aB). Paralog of RPL23aA
ELF5A-3	AT1G69410.1	Eukaryotic translation initiation factor 5A-3
AT2G34480	AT2G34480.1	Ribosomal protein L18ae/LX family protein
AT5G27850	AT5G27850.1	Ribosomal protein L18e/L15 superfamily protein
AT1G73230	AT1G73230.1	Nascent polypeptide-associated complex NAC
AT4G25740	AT4G25740.1	RNA binding Plectin/S10 domain-containing protein
AT1G09640	AT1G09640.1	Translation elongation factor EF1B, gamma chain
TCTP	AT3G16640.1	Encodes a protein homologous to translationally controlled tumor protein (TCTP) from Drosophila
ABCF3	AT1G64550.1	Member of GCN subfamily; Belongs to the ABC transporter superfamily.
AT1G07920	AT1G07930.1	GTP binding Elongation factor Tu family protein
AAC3	AT4G28390.1	Encodes a mitochondrial ADP/ATP carrier protein
WEE1	AT1G02970.1	Wee1-like protein kinase
AT1G30580	AT1G30580.1	Obg-like ATPase 1; Hydrolyzes ATP, and can also hydrolyze GTP with lower efficiency
UAP56a	AT5G11170.1	DEAD/DEAH box RNA helicase family protein
AT4G26310	AT4G26310.2	Elongation factor P (EF-P) family protein

TPI	AT3G55440.1	Triosephosphate isomerase, cytosolic; Encodes triosephosphate isomerase
TCP-1	AT3G20050.1	T-complex protein 1 alpha subunit; Molecular chaperone
eEF-1Bb1	AT1G30230.2	Glutathione S-transferase, C-terminal-like;Translation elongation factor EF1B/ribosomal protein S6
AT2G18110	AT2G18110.1	Translation elongation factor EF1B/ribosomal protein S6 family protein
ATKRS-1	AT3G11710.1	Lysine–tRNA ligase, cytoplasmic
ORC3	AT5G16690.1	Origin Recognition Complex subunit 3. Involved in the initiation of DNA replication
MCM5	AT2G07690.1	Minichromosome maintenance (MCM2/3/5) family protein
ETG1	AT2G40550.1	Mini-chromosome maintenance complex-binding protein
PLE	AT5G51600.1	Microtubule associated protein (MAP65/ASE1) family protein
ATK1	AT4G21270.1	Kinesin-like protein KIN-14C
CYCA3;1	AT5G43080.1	Putative cyclin-A3-1; Cyclin A3;1 (CYCA3;1)
RNR1	AT2G21790.1	Ribonucleoside-diphosphate reductase large subunit
HTA9	AT1G52740.1	Probable histone H2A variant 3
UBC19	AT3G20060.1	Encodes one of two ubiquitin-conjugating enzymes belonging to the E2-C gene family
AT3G42660	AT3G42660.1	Transducin family protein / WD-40 repeat family protein
CDKB2;2	AT1G20930.1	Cyclin-dependent kinase
CHR1	AT5G66750.1	ATP-dependent DNA helicase DDM1
AT4G28310	AT4G28310.1	Uncharacterized protein At4g28310; Unknown protein
ORC6	AT1G26840.1	Origin of replication complex subunit 6
MCM3	AT5G46280.1	Minichromosome maintenance (MCM2/3/5) family protein
MAP65-8	AT1G27920.1	Microtubule-associated protein 65-8 (MAP65-8)
AT1G09200	AT5G10390.1	Histone superfamily protein; Core component of nucleosome
MCM2	AT1G44900.1	Minichromosome maintenance (MCM2/3/5) family protein
BRCA1	AT4G21070.1	Encodes AtBRCA1, an ortholog of the human breast cancer susceptibility gene 1
CYCA1;1	AT1G44110.1	Cyclin A1;1 (CYCA1;1
MCM10	AT2G20980.1	Minichromosome maintenance 10

AT1G14300	AT1G14300.2	ARM repeat superfamily protein
AT5G01230	AT5G01230.1	S-adenosyl-L-methionine-dependent methyltransferases superfamily protein
NRPC2	AT5G45140.1	DNA-directed RNA polymerase III subunit 2
emb2742	AT3G12670.1	CTP synthase family protein
AT1G48570	AT1G48570.1	Zinc finger (Ran-binding) family protein
AT4G02400	AT4G02400.1	U3 ribonucleoprotein (Utp) family protein
AT4G23540	AT4G23540.1	ARM repeat superfamily protein; Its function is described as binding
AT5G11240	AT5G11240.1	Transducin family protein / WD-40 repeat family protein
TTN5	AT2G18390.1	ADP-ribosylation factor family protein
CMT3	AT1G69770.1	DNA (cytosine-5)-methyltransferase CMT3
AT1G63100	AT1G63100.1	GRAS family transcription factor
VAM3	AT5G46860.1	Syntaxin/t-SNARE family protein
ENODL14	AT2G25060.1	Early nodulin-like protein 14 (ENODL14)
SYP111	AT1G08560.1	Syntaxin-related protein KNOLLE
AT5G16250	AT5G16250.1	Uncharacterized protein T21H19_170
CSLD5	AT1G02730.1	Cellulose synthase-like protein D5
PER64	AT5G42180.1	Peroxidase superfamily protein
RCI3	AT1G05260.1	Peroxidase superfamily protein
AT5G66390	AT5G66390.1	Peroxidase superfamily protein
CAD9	AT4G39330.1	Probable cinnamyl alcohol dehydrogenase 9
PRX52	AT5G05340.1	Peroxidase superfamily protein

Additional Files

Additional file 1: Figure S1 PCA graph of 2 dpi treatment and control treatment. The graph analyzes the spatial dispersion between treatment and control and their respective replicas

Additional file 2: Figure S2 PCA graph of 10 dpi treatment and control treatment. The graph analyzes the spatial dispersion between treatment and control and their respective replicas

Additional file 3: Table S1 Statistics of sequencing and filtering of raw data

Additional file 4: Figure S3 Annotation all unigenes derived from the *de novo* transcriptome assembly of *V. planifolia* upon infection by *Fov*. Annotation was based on Gene Ontology terms using Blast2GO. GO categories are as follow: biological process (BP), molecular function (MF), and cellular component (CC). The number of genes corresponding to each functional category is shown

Additional file 5: Table S2 Assembly statistics and sequence mapping

Additional file 6: Table S3 DEGs at 2 and 10 dpi obtained with several methods, including DESeq, DESeq2, NOISeq and EdgeR

Additional file 7: Table S4 Functional annotation of DEGs at 2 and 10 dpi obtained with the EdgeR method

Additional file 8: Figure S4 Schematic representation of biological processes enriched in DEGs at 2 dpi. **a** Biological processes enriched among up-regulated genes. **b** Biological processes enriched among down-regulated genes. Enrichment analysis was performed with agriGO. Enriched GO terms considered as significant are indicated by corresponding color levels

Additional file 9: Figure S5 Functional association networks among DEGs at 10 dpi. **a** Interactions among the up-regulated genes. **b** Interactions among the down-regulated genes. Colored lines between nodes indicate the various types of interaction: black line, co-expression; light blue line, association in curated databases; purple line, experimental

Figures

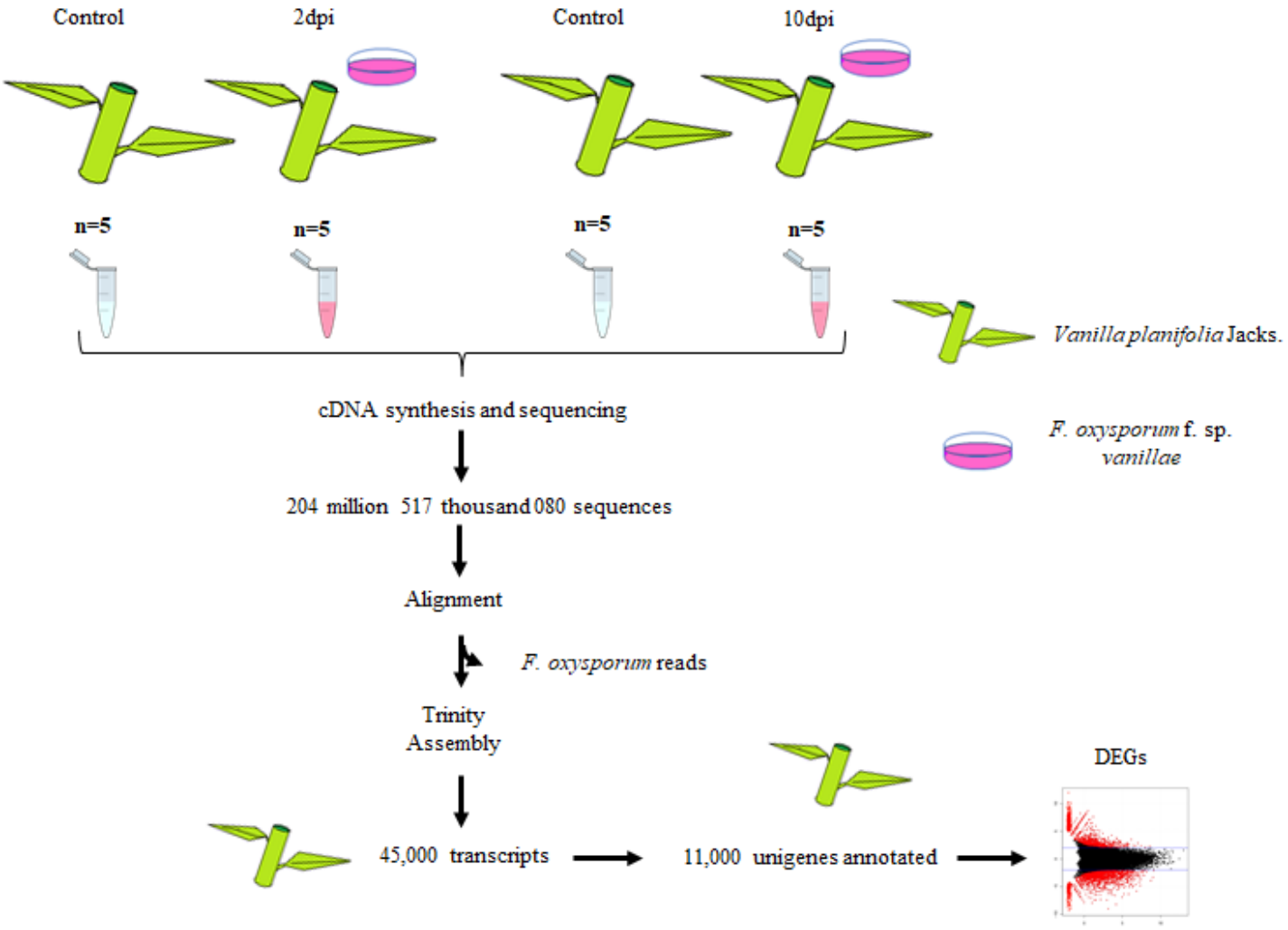

Figure 1

1 Flow diagram outlining the experimental design and key steps in the process of the de novo transcriptome assembly for V. planifolia plants upon infection by Fov. Total RNA from non-treated (Control; C) and treated (2 and 10 dpi) plants were converted to cDNA and subjected to high- throughput sequencing. For details, see Materials and Methods1 Flow diagram outlining the experimental design and key steps in the process of the de novo transcriptome assembly for V. planifolia plants upon infection by Fov. Total RNA from non-treated (Control; C) and treated (2 and 10 dpi) plants were converted to cDNA and subjected to high- throughput sequencing. For details, see Materials and Methods

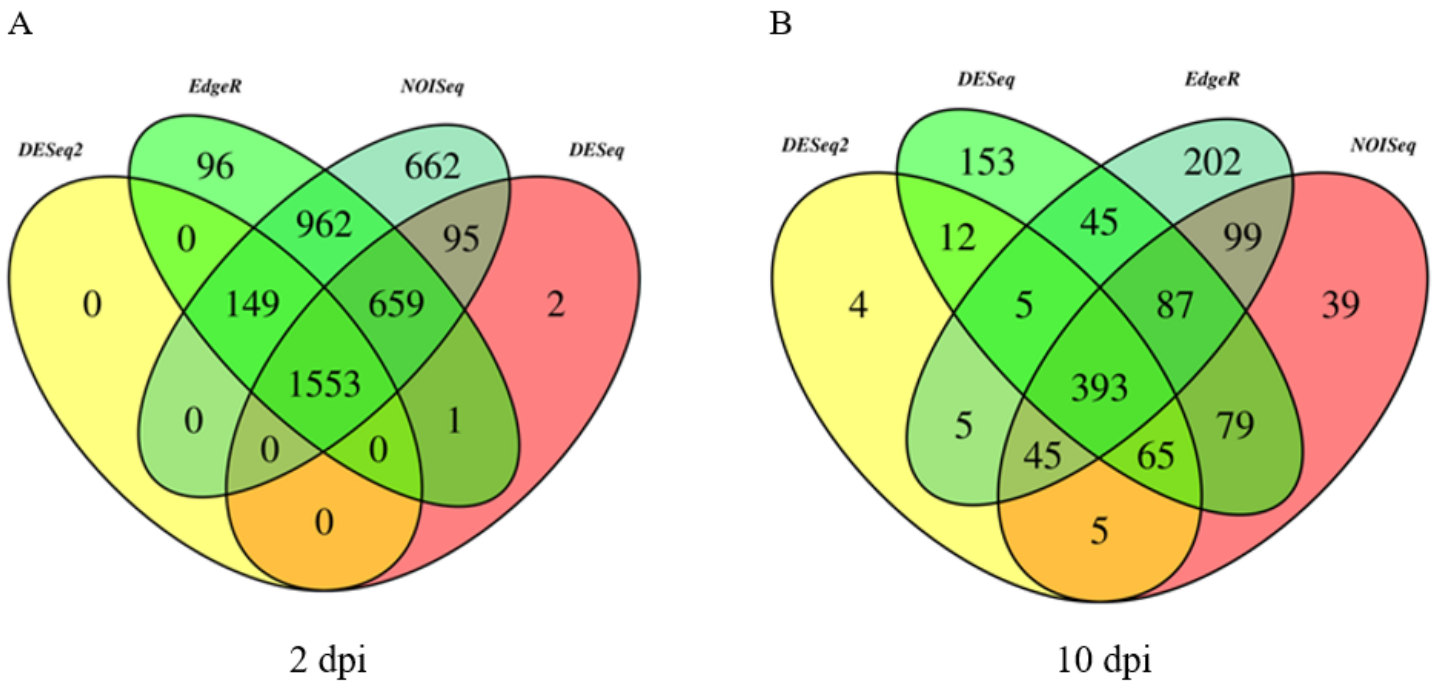

Figure 2

Venn diagrams showing the degree of overlap between DEGs obtained with different methods. a Number of DEGs obtained by DESeq, DESeq2, NOISeq and EdgeR for data set at 2 dpi. b Number of DEGs obtained for data set at 10 dpi with the same methods as shown in a. Results from each method are shown with different colors

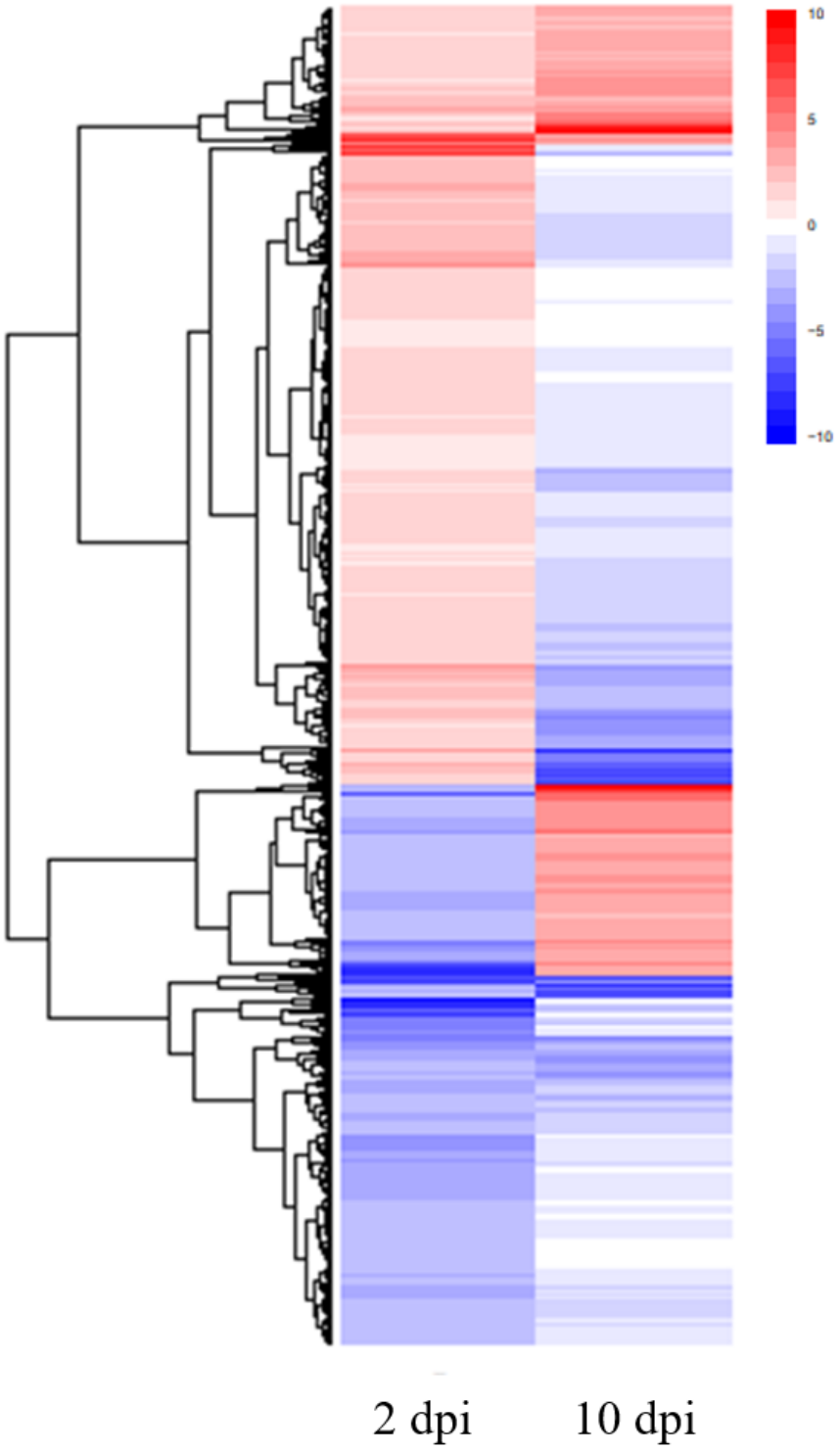

Figure 3

Overall expression patterns of DEGs at 2 and 10 dpi. Heat maps of data sets at 2 (3420 DEGs) and 10 dpi (881 DEGs) are shown. The heat maps were made using the ggplot2 included in R package [81]

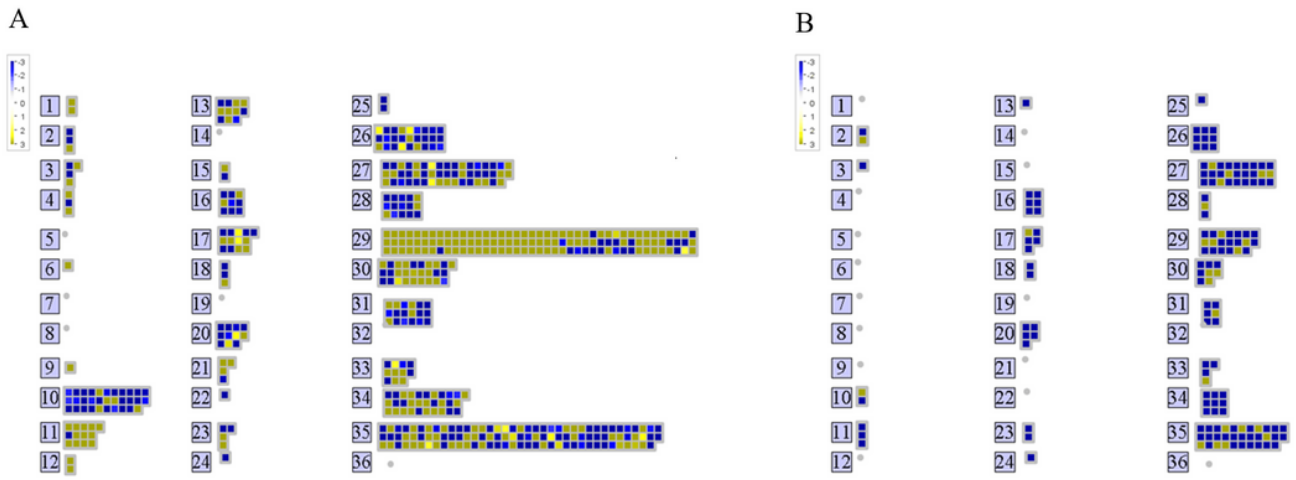

Figure 4

MapMan analysis of DEGs showing their expression profiles at 2 and 10 dpi. a Heat map of DEGs at 2 dpi. b Heat map of DEGs at 10 dpi. The numbers correspond to different MapMan functional categories of gene ontology as described below: 1 PS, 2, major CHO metabolism, 3 minor CHO metabolism, 4 glycolysis, 6 gluconeogenese/glyoxylate cycle, 9 mitochondrial electron transport/ATP synthesis, 10 cell wall, 11 lipid metabolism, 12 N-metabolism, 13 amino acid metabolism, 15 metal handling, 16 secondary metabolism, 17 hormone metabolism, 18 Co-factor and vitamin metabolism, 20 stress, 21 redox, 22 polyamine metabolism, 23 nucleotide metabolism, 24 Biodegradation of Xenobiotics, 25 C1-metabolism, 26 misc, 27 RNA, 28 DNA, 29 protein, 30 signaling, 31 cell, 33 development, 34 transport, 35 not assigned

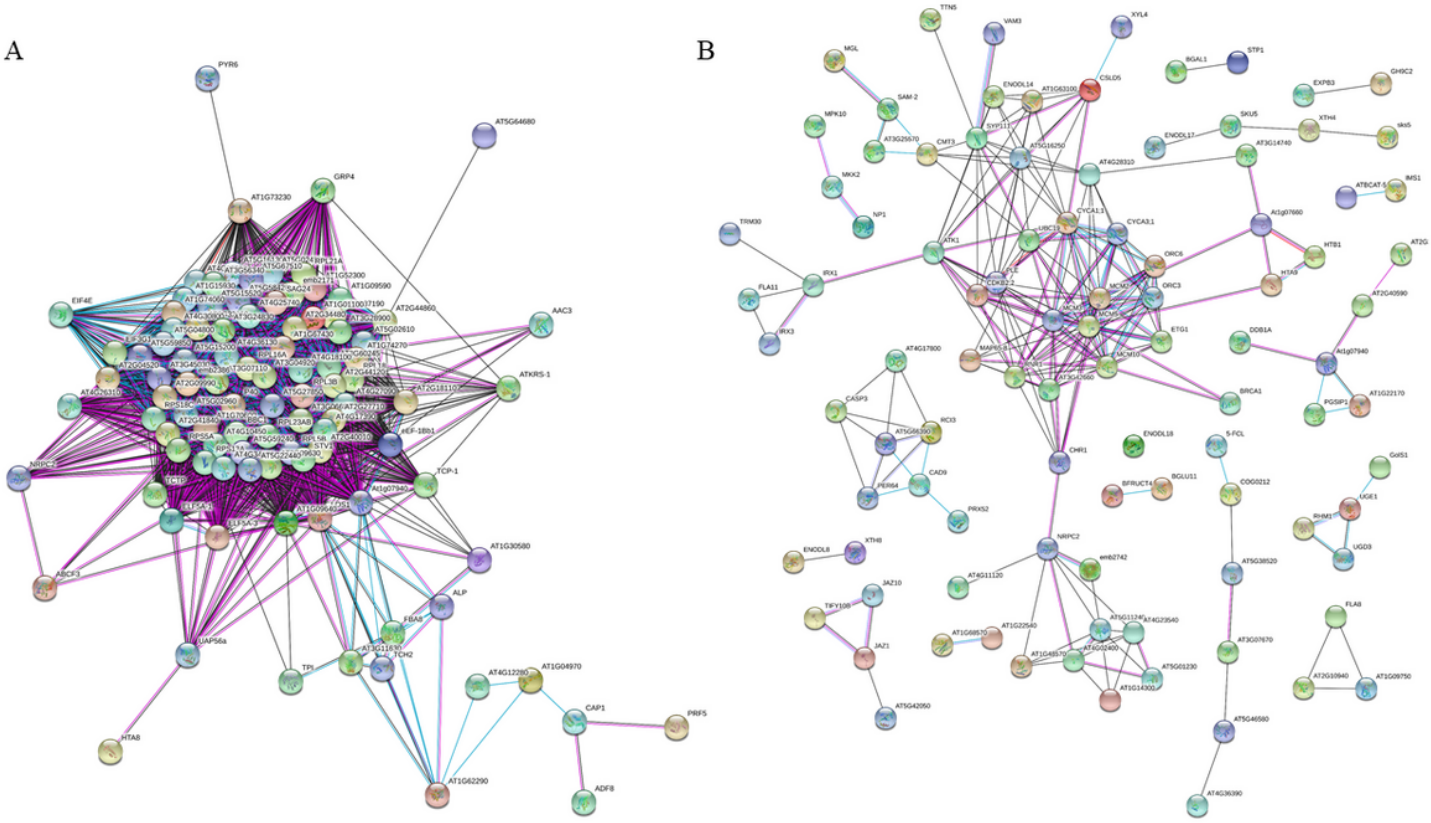

Figure 5

Functional association networks among DEGs corresponding to 2 dpi. a Interactions among the up-regulated genes obtained with the STRING software [35]. b Interactions among the down-regulated genes. Colored lines between nodes indicate the various types of interaction: black line, co-expression; light blue line, association in curated databases; purple line, experimental

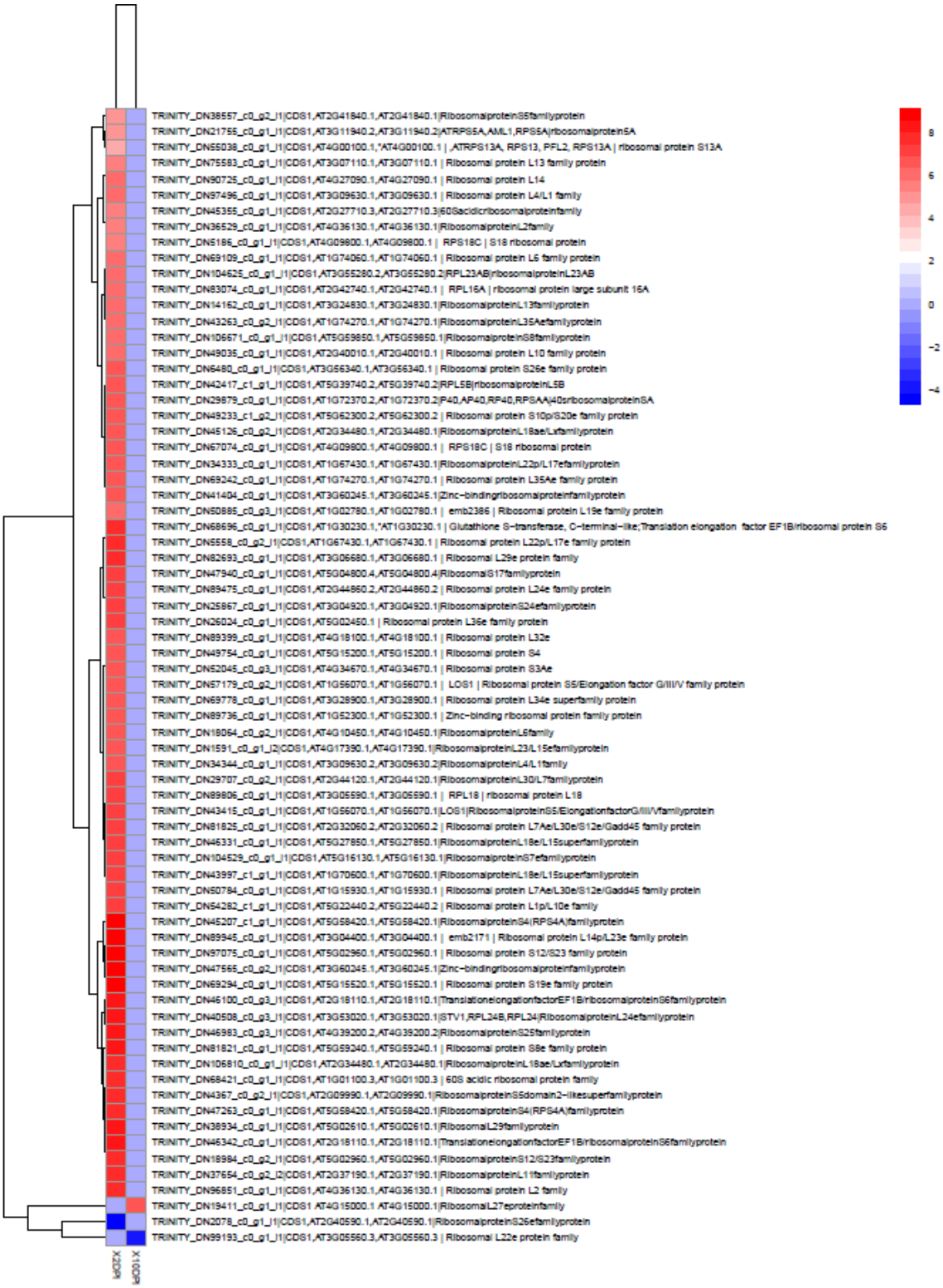

Figure 6

Heat map of ribosomal proteins comparing datasets of 2 and 10 dpi. The heat maps were made using the ggplot2 included in R package [81]

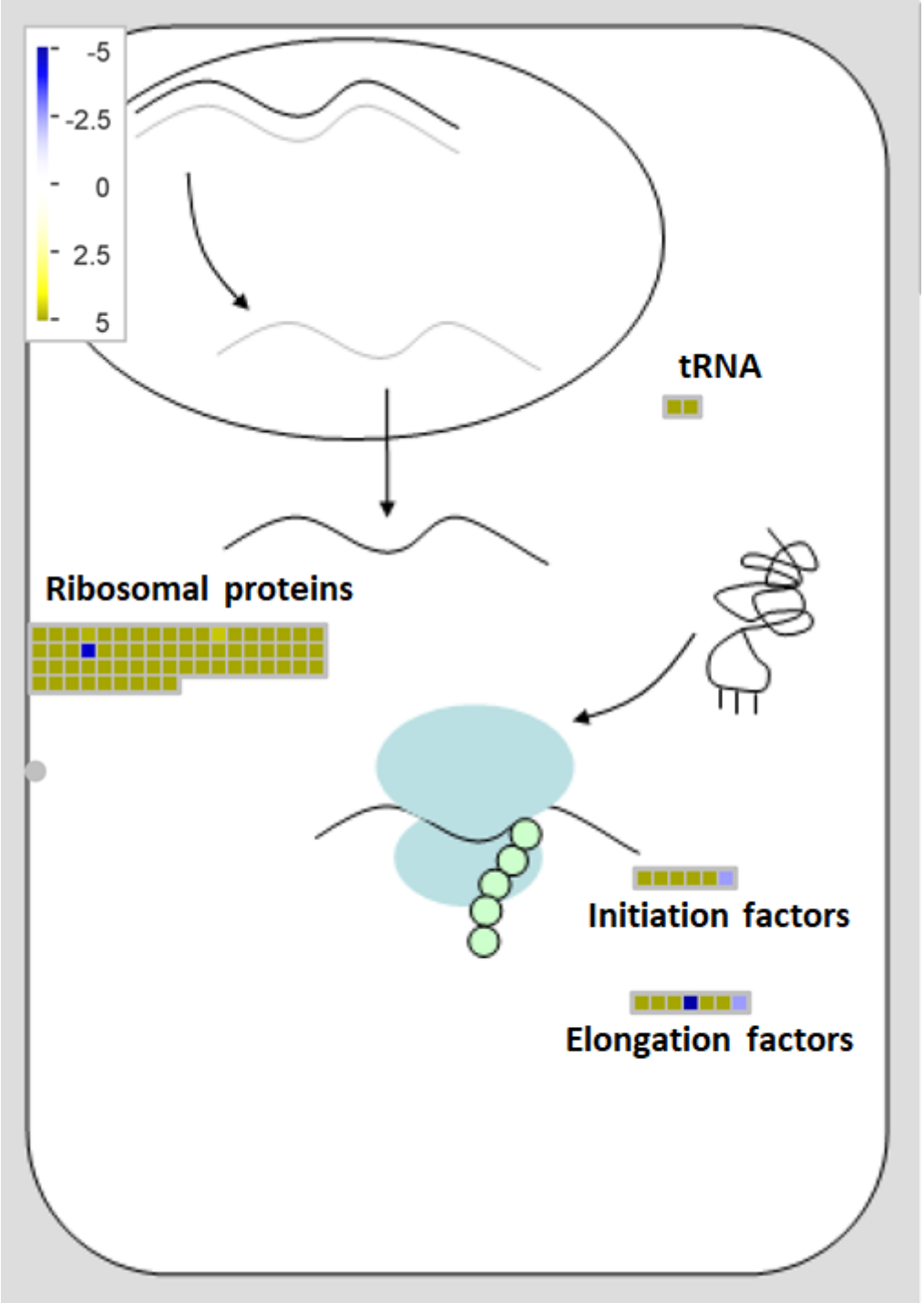

Figure 7

Overview of MapMan RNA-protein synthesis at 2 dpi. Transcript levels of translation-related genes (RPs, tRNAs, initiation factors and elongation factors) are shown. Upon invasion by Fov, induction of RPs leads to changes in ribosome composition, driving to selective translation of certain transcripts

Supplementary Files

This is a list of supplementary files associated with this preprint. Click to download.

- Additionalfile3TableS1.xlsx
- Additionalfile6TableS3.xlsx
- Additionalfile7TableS4.xlsx
- Additionalfile4FigureS3.png
- Additionalfile1FigureS1.png
- Additionalfile8FigureS4.png
- Additionalfile5TableS2.xlsx
- Additionalfile2FigureS2.png
- Additionalfile9FigureS5.png